

Thickness-Dependent Topological Surface States on Sb (111) Thin Films

Yao Guanggeng, Pan Feng, Luo Ziyu, Xu Wentao, Feng Yuanping, Andrew Thye Shen Wee, Wang Xue-sen

Department of Physics, National University of Singapore

[Introduction]

Motivated by the unique electronic properties of antimony (Sb) and its fascinating potential in the area of topological insulators (TIs), Sb films were investigated using *in-situ* STM/STS. More specifically, there are several reasons why we choose this topologically nontrivial system:

1. Although Sb is semimetal in bulk due to its negative indirect bandgap, it has a vital band inversion at L point. Sb(111) has been confirmed to possess **topological surface states** (TSSs), leading to the absence of 180° backscattering due to protection of time-reversal (TR) symmetry.

2. The strongly **distorted Dirac cone** of TSS on Sb(111) can create various scattering channels in QPI patterns, from which the spin information of TSS might be extracted. Measuring the patterns at different film thickness helps us understand the evolution of spin texture as inter-surface coupling varies.

3. Thin films with **larger surface-to-volume ratios** than bulk materials can manifest the surface effect significantly, giving a larger contribution from the surface and making it more observable.

4. Compared with the well-studied compound TIs such as Bi_2Se_3 , Sb is a **single-element** simple system, and hence Sb thin films may provide a straightforward demonstration for topological properties without considering the residual bulk carriers from self-doping states or spatial fluctuations of charge and spin helicity.

Taking advantage of the STM/STS and DFT simulations, we obtained the **quasi-particle interference** (QPI) patterns and proved that as the film thickness decreases, part of TSSs degenerate to quantum well states (QWSs) and lose their topological properties. The key scattering processes were explored on several representative thicknesses, demonstrating the thickness-dependent competing process between the intra-surface and inter-surface coupling effects.

[Results and Discussion]

1. Atomic and Band Structure of Sb (111)

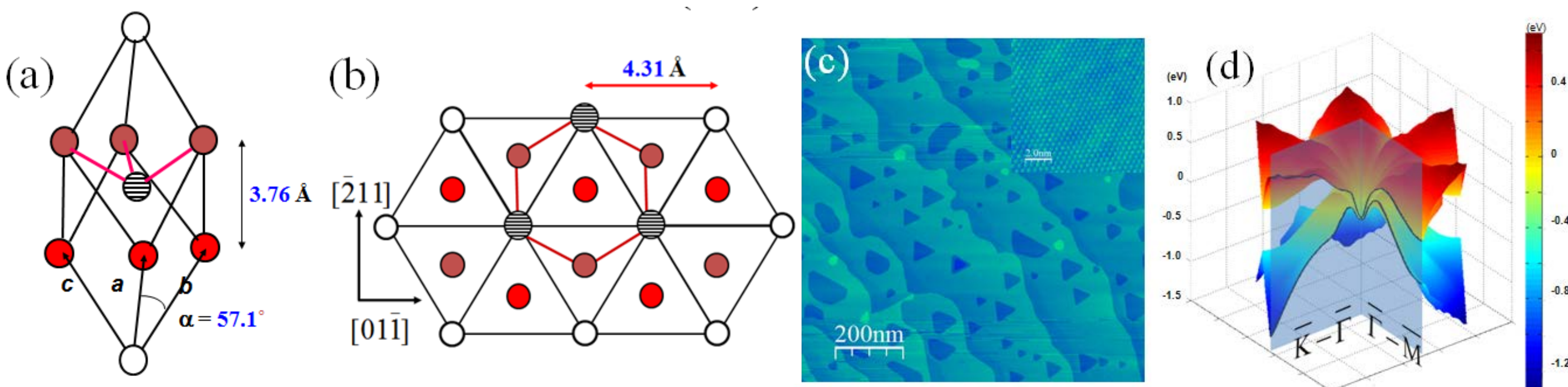


Fig. 1 (a) Schematic of the unit cell of rhombohedral Sb lattice. (b) Schematic of Sb (111) with in-plane atomic period of 4.31 \AA . (c) STM topography of 30-BL Sb(111) film. The insets shows the atomic-resolution image. (d) Calculated Sb (111) surface bands with two cuts (shown as black lines) along high symmetry directions $\bar{\Gamma}-\bar{M}$ and $\bar{\Gamma}-\bar{K}$, which form the distorted Dirac cone around $\bar{\Gamma}$.

2. QPI on 30-BL Sb (111)

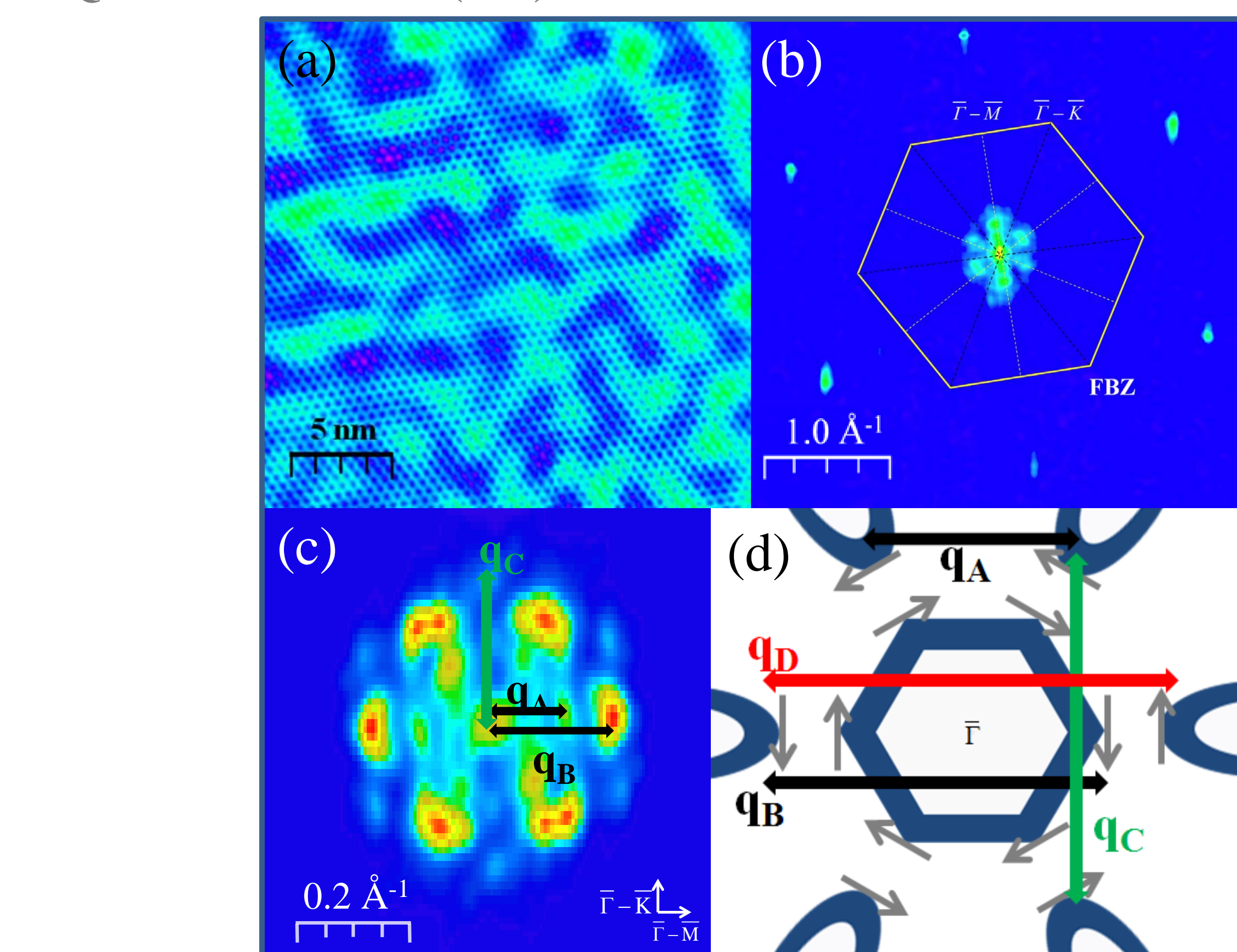


Fig. 2 (a) Real-space image shows coexistence of atomic resolution and QPI patterns on 30-BL Sb(111). (b) FT-STS pattern of (a), consisting of six strong peaks along $\bar{\Gamma}-\bar{M}$. The FBZ (yellow hexagon) as well as the high symmetry directions is marked. (c) Zoom-in of FT-STS pattern around $\bar{\Gamma}$ with three observable scattering vectors \mathbf{q}_A , \mathbf{q}_B and \mathbf{q}_C . (d) Schematic of CEC as well as the spin texture around $\bar{\Gamma}$, which has a central electron pocket and six hole pockets. The small grey arrows represent the spin directions. \mathbf{q}_A and \mathbf{q}_B are allowed scattering vectors, while \mathbf{q}_C with a much less probability and \mathbf{q}_D total forbidden.

3. Dispersion Relationship and Simulation for 30-BL Sb (111)

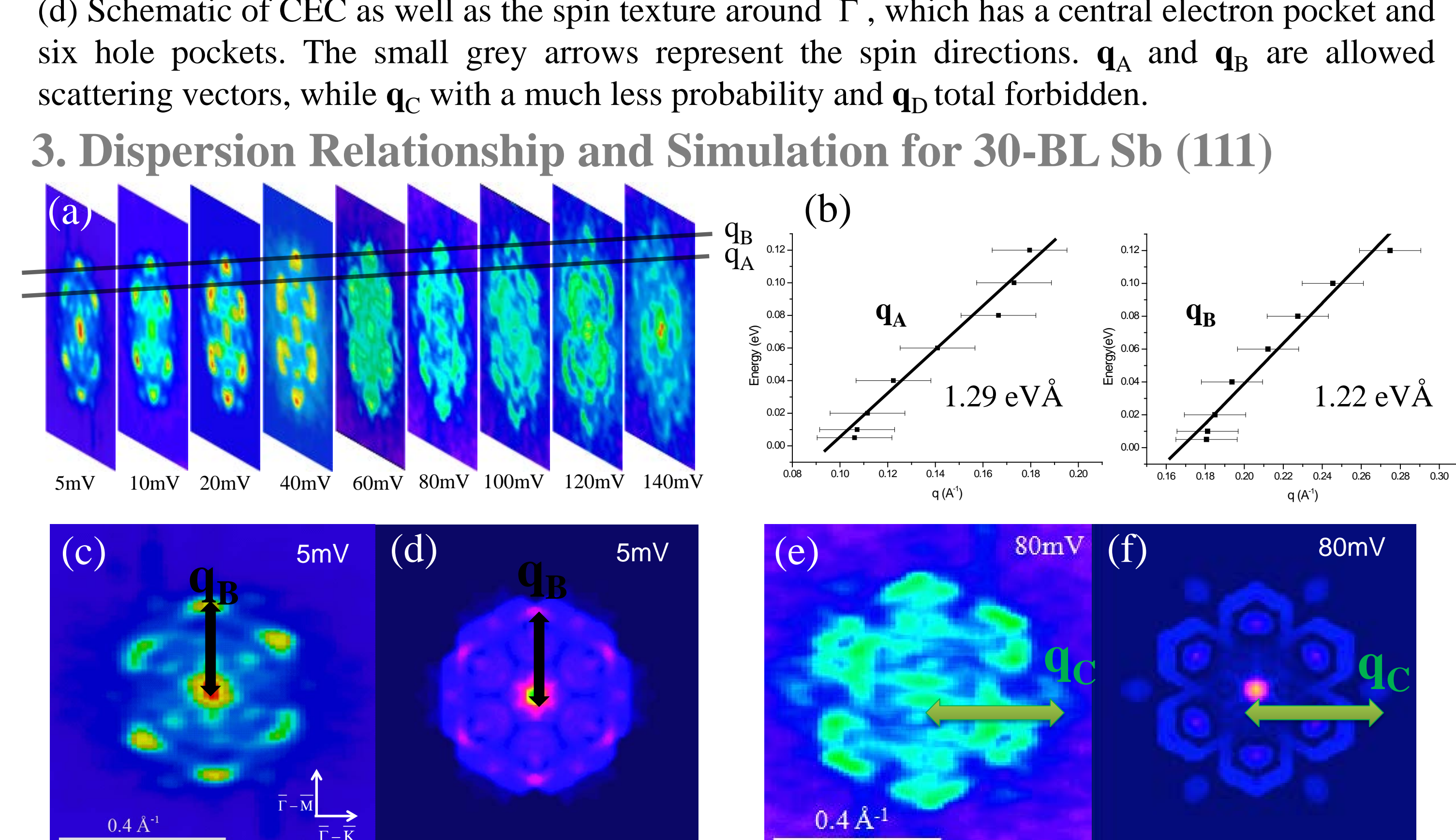


Fig. 3 (a) Linear dispersion based on FT-STS maps of the same area at bias from 5mV to 140mV . Each map shows two sets of scattering vectors corresponding to \mathbf{q}_A and \mathbf{q}_B , respectively. (b) The slopes of \mathbf{q}_A and \mathbf{q}_B extracted from (a). Here the error bar corresponds to $0.05\pi \text{ \AA}^{-1}$. (c-d) At 5mV the FT-STS mapping (c) and the corresponding calculated QPI patterns (d). (e-f) At 80mV the FT-STS mapping (e) and the corresponding calculated QPI patterns (f). \mathbf{q}_B and \mathbf{q}_C are marked for comparison with Fig.2 (c-d).

4. QPI on 9-BL Sb (111)

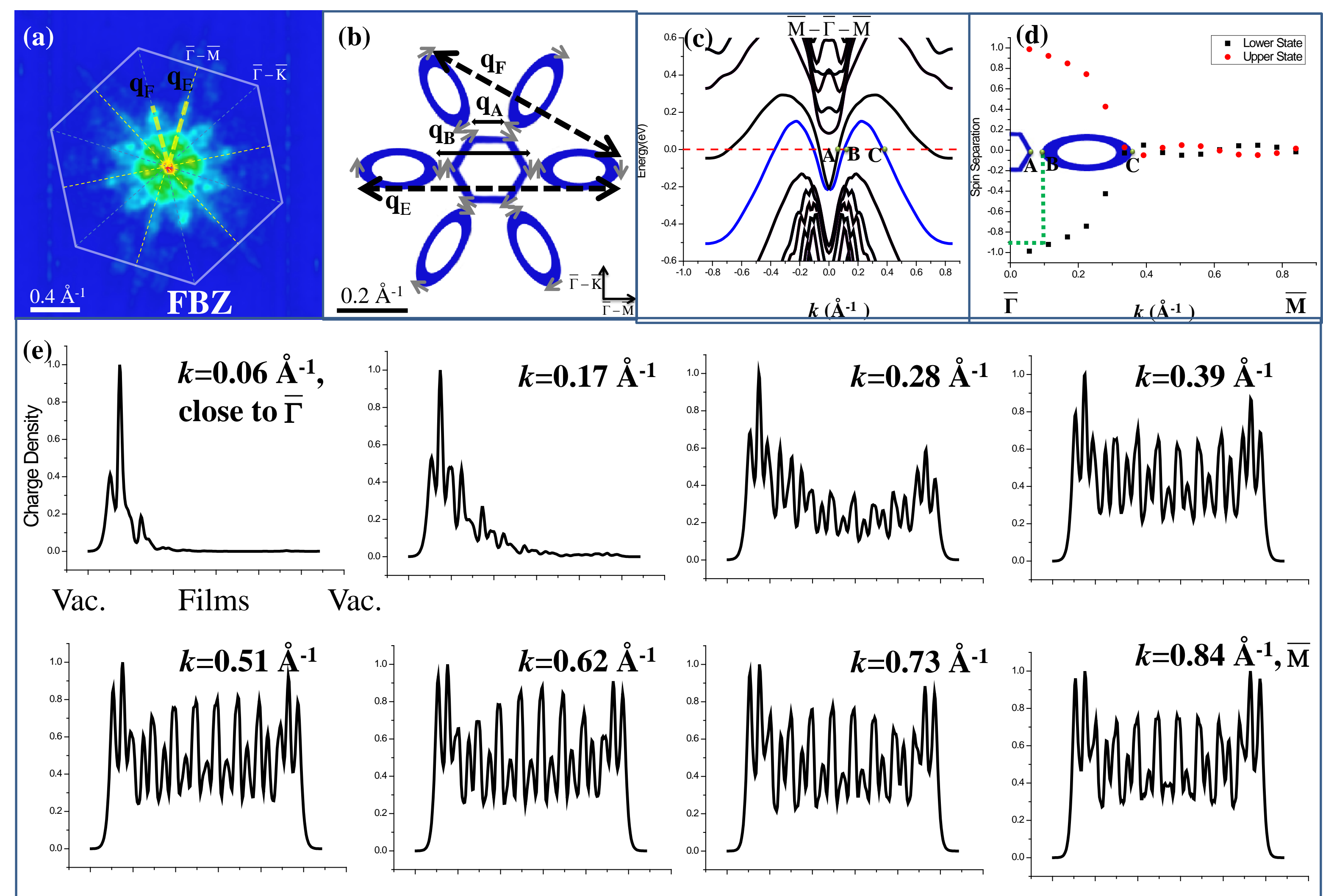


Fig. 4 (a) FT-STS mapping at 20mV . Two cutoff vectors (\mathbf{q}_E and \mathbf{q}_F) are shown as yellow dashed lines. (b) \mathbf{q}_E and \mathbf{q}_F in the calculated CEC at Fermi energy. The grey arrows illustrate the spin directions on the upper surface. Obeying spin conservation, \mathbf{q}_A and \mathbf{q}_B (solid black lines) still exist and correspond to the central green zone with high intensities in (a). (c) Calculated band structure of 9-BL Sb(111) along $\bar{M}-\bar{\Gamma}-\bar{M}$. The blue lines represent the surface band chosen for computing the spin separation. (d) Spin separation as a function of the wavevector, indicating the strong k -dependent coupling of upper and lower states. A, B and C points are labeled for comparison between the band structure and CEC. (e) The real-space distribution of SS from near $\bar{\Gamma}$ to \bar{M} obtained from DFT computation, showing that a well-defined localization of SS around $\bar{\Gamma}$ but large penetration depth for states from 0.34 \AA^{-1} to \bar{M} , which is strong evidence to treat that part of states as QWSs.

5. Thickness-Dependent QPI on Sb (111)

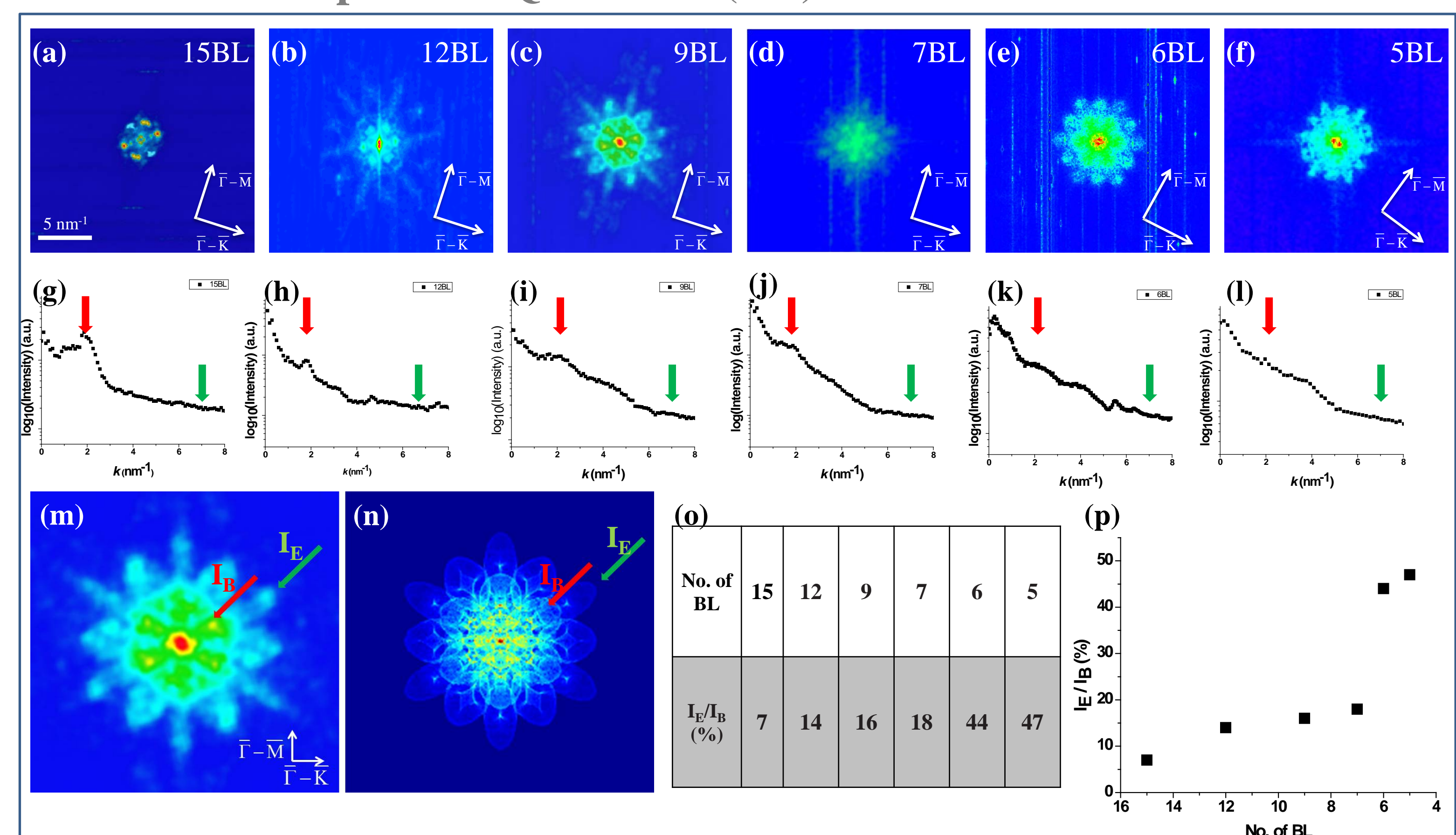


Fig. 5 (a-f) FT-STS mapping taken at $+20\text{mV}$ on 15, 12, 9, 7, 6, 5BL Sb(111), respectively. (g-l) Corresponding average intensities (logarithmic scale) along $\bar{\Gamma}-\bar{M}$. The red and green arrows mark the intensity I_B due to intra-surface coupling and I_E due to inter-surface coupling. (m-n) FT-STS mapping (m) and the corresponding calculated QPI patterns (n). (o-p) Ratio I_E/I_B vs. the film thickness. The ratio increases monotonically as the film becomes thinner.

[Conclusions]

The inter-surface coupling of TSSs in Bi_2Se_3 thin films has been studied both theoretically and experimentally. Comparing to Sb(111), TSSs on Bi_2Se_3 form a fairly ideal Dirac cone with rather weak warping in the bulk bandgap region, so they can be considered as true surface states. Sb(111) has a highly warped Dirac cone. From the $\bar{\Gamma}$ point to \bar{M} , "SSs" penetrate deeper and deeper into the interior. Additionally, when the film is thinner, the inter-surface coupling of these states makes them located more near the film centre than at the surfaces. The spin splitting due to the Rashba effect is greatly diminished, indicating a thickness-dependent process of diminishing spin polarization.

Although not an ideal TI, Sb(111) ultrathin films allow us to investigate the extraordinary scatterings between SSs with nearly parallel spin directions, while in other TIs possessing an ideal Dirac cone it is impossible to get similar features exclusively between SSs. The "distorted" Dirac cone and dramatic **momentum/thickness-dependent** penetration depth of SSs offer us an interesting quasi-2D system to help interpret the detailed evolution of coupling and hybridization of TSSs. Of particular interest is the tunability of contributions of inter-surface scatterings relative to those of intra-surface by means of changing thicknesses, which can influence the transport properties from the application point of view.